NJC

Accepted Manuscript

This is an *Accepted Manuscript*, which has been through the Royal Society of Chemistry peer review process and has been accepted for publication.

Accepted Manuscripts are published online shortly after acceptance, before technical editing, formatting and proof reading. Using this free service, authors can make their results available to the community, in citable form, before we publish the edited article. We will replace this *Accepted Manuscript* with the edited and formatted *Advance Article* as soon as it is available.

You can find more information about *Accepted Manuscripts* in the Information for Authors.

Please note that technical editing may introduce minor changes to the text and/or graphics, which may alter content. The journal's standard Terms & Conditions and the Ethical guidelines still apply. In no event shall the Royal Society of Chemistry be held responsible for any errors or omissions in this *Accepted Manuscript* or any consequences arising from the use of any information it contains.

ROYAL SOCIETY OF CHEMISTRY

www.rsc.org/njc

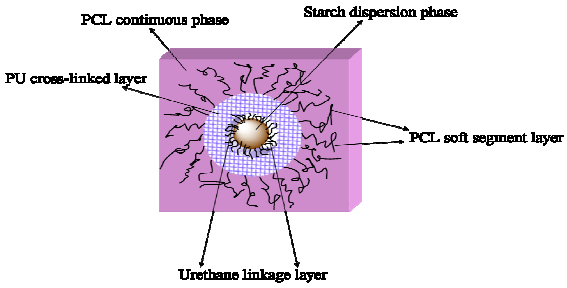

A novel polyurethane prepolymer compatibilizer successfully improved the compatibility and performances of polycaprolactone (PCL)/starch composites.

Effects of a Novel Compatible Interface Structure on the Properties of Starch-PCL Composites

Jingjing Liao, Zimu Luo, Yu Zhang, Xu Zhang, Jing Cheng, Qiangxian Wu*

Green Polymer Laboratory, College of Chemistry, Central China Normal University, Wuhan, China, 430079

ABSTRACT:

Polycaprolactone (PCL)/starch composites were prepared in an intensive mixer using PCL-based polyurethane prepolymer (PCLPU) as a compatibilizer. A multifunctional polyurethane layer (PCLPU layer) was then located at the interface between the starch granules and PCL matrix. Good compatibility was shown between starch and PCLPU layer, which was attributed to the urethane linkages. And the degradation experiment revealed that the urethane linkages between PCLPU and starch were stable. The PCL soft segments in PCLPU layer could also interact with PCL matrix through PCL crystallinity to improve the compatibility between PCL matrix and PCLPU. The multifunctional PCLPU was thus deemed effective in improving the compatibility of starch-PCL composites. Additionally, the mechanical properties and thermal stability of the composites enhanced compared to starch-PCL composites. The novel

* Corresponding author at: College of Chemistry, Central China Normal University, Wuhan, China, 430079. Tel. and fax: +86-27-67867953;

E-mail address: greenpolymerlab@yahoo.com (Q. X. Wu).

multifunctional PCLPU layer therefore played an important role in improving the compatibility between the starch and PCL and the properties of starch-PCL composites.

Keywords: Starch; Polycaprolactone; Polyurethane; Compatibility; Biodegradable

Introduction

In the last two decades, the increased production and use of plastic materials has led to an urgent need for waste disposal solutions.[1] Biodegradable polymers and composites have been considered as one of the solutions to the public environmental problem caused by the waste disposal of traditional nondegradable polymers.[2-4] Starch, being an important set of natural biopolymers, has been considered as one of the most promising candidate materials due to its biodegradability, derivability, availability, and low cost.[5-8] However, native starch is very hydrophilic and possesses inferior mechanical properties compared with most polymers. To overcome these issues, various physical and chemical modifications of starch granules have been considered. To obtain completely biodegradable materials, starch is blended with various biodegradable polymers.[9] Among the many kinds of candidates, the composites of starch and aliphatic polyester, especially PCL, can reach the goal.[10-14] However, the poor miscibility between hydrophilic starch and hydrophobic PCL has been a difficulty to be overcome for enhancement of the properties of the composites.[15]

Much previous research has focused on compatibilizing the composites of PCL and starch. Various compatibilizers and additives have been proposed to improve the interface between starch and biodegradable polyesters.[16-18] In recent years, PCL-g-

glycidyl methacrylate (PCL-g-GMA) and PCL-g-diethyl maleate (PCL-g-DEM), as reactive interfacial agents for starch-PCL systems, were utilized to improve the compatibility and so the adhesion between the two immiscible polymers.[19] These compounds were prepared by reacting a low molecular weight PCL (M_w=3000) with GMA or DEM in the presence of benzoylperoxide (BPO) at 130 °C. The mechanical properties of the compatibilized blends differ from the uncompatibilized ones and in particular the elastic modulus for the compatibilized blends was found significantly higher. It is also confirmed that poly (ethylene glycol) (PEG) which has an appropriate molecular weight is the most commonly used compatibilizer and the most widely researched for starch-based composites. PEG is able to interact with both the starch phase and the PCL phase by locating at the interface and stabilize the starch-PCL composites.[20,21] Evidently, various compatibilizers have been used to improve interfacial compatibility and performances of starch-PCL composites. However, the compatibilizers such as maleate or maleic anhydride are not easy to react with starch with high efficiency, which result in limited compatibility between starch and hydrophobic polymer.

Polyurethanes,[22] first discovered in the 1940s, attracted much research attention due to their versatile applications and the possibility to be synthesized with a wide variety of isocyanates and polyols.[23] The reaction leads to a unique polyurethane that

is generally composed of polyether or polyester soft segments and diisocyanate-based hard segments.[24] A wide range of materials can be used in the preparation of PUs and as such, the subsequent polymers can have a wide range of properties.[25] In our previous work, PCLPU was used to prepare modified starch.[26] A grafting ratio of near 100% was demonstrated for PUP modified starch, which was attributed to the high reactivity between the isocyanate groups of PUP and the hydroxyl groups of starch.[27] The properties of the modified starch were thus improved compared with pure starch materials. Namely, the PCLPU demonstrated good compatibility with starch through urethane linkages. Moreover, the PCLPU and the PCL matrix showed good compatibility because they both had PCL crystal component. It was therefore supposed that a novel compatible PCLPU layer structure could be formed to improve the compatibility of starch and PCL matrix. The multifunctional PCLPU has thus been proposed as a compatibilizer for the preparation of starch-PCL composites. This endeavor was not tried in our previous work and much remains to be explored in this area.

In this work, polycaprolactone (PCL)/starch composites were prepared in an intensive mixer using polyurethane prepolymer which was synthesized with PCL diol and 4, 4′-methylenedi-*p*-phenyl diisocyanate (MDI) as a compatibilizer. The effects of the novel compatibilizer on the structure and properties of the starch-PCL composites

were investigated.

Experimental

Materials

Polycaprolactone (M_w=65000 g mol^{-1}) and polycaprolactone diol (M_w=2000 g mol^{-1}, hydroxyl value=57.52mg KOH g^{-1}) were purchased from Perstorp UK Ltd. (Cheshire, UK). 4,4'-methylenedi-*p*-phenyl diisocyanate (MDI, 98%) were purchased from Sigma-Aldrich Fine Chemicals (St. Louis, MO, USA). Corn starch (CS, amylose:23–26 wt.%; moisture: 12 wt.%) was obtained from Wuhan Corn Starch CO. Ltd. (Wuhan, China) and used without any further pretreatments. High-temperature amylase (activity: 20000 u/mL) and α−Amylase (activity: 100000 u/g) were obtained from Jienuo Enzyme Co. Ltd. (Zaozhuang, China) and acetone (analysis grade) was purchased from the China National Pharmaceutical Group Corporation (Shanghai, China).

Synthesis of PUP

The molar number ratio of isocyanate to hydroxyl group (NCO/OH) was 2.0. Polycaprolactone diol (160 g) was charged into a 250 mL three-necked flask fitted with a stirrer operating at a speed of 300 rpm, an inlet and an outlet. The system was dried in vacuum at 100 °C to remove the moisture in the PCL diol. After 30 min, the temperature of the PCL diol in the flask was decreased to 70 °C and MDI (40 g) was

then charged into the flask under vacuum conditions. The translucent mixture in the flask quickly became transparent. Fifteen minutes after the addition of MDI, the mixture was stirred vigorously and reacted at 80 °C for 1 h. Finally, a white PUP solid was obtained.

Preparation of PU powder

PU powder (PW) here was a control sample for PUP. The PCLPU was soaked in water for 2 days. In this case, the un-reacted terminal NCO groups of the PUP were consumed by water and then mill the PUP sheet into PU powder in a polymer grinder (GP-00001 model, Wuhan Qien Science & Technology Co., Ltd., Wuhan, China) with the use of liquid nitrogen. The PU powder was then filtered using a screen with 80 meshes.

Preparation of Starch-PCL composites

Corn starch (49 g), PCLPU (7 g) and PCL (14 g) were charged into an intensive mixer (SU-70, Changzhou Suyan Science and Technology Co., Ltd., Changzhou city, China) and mixed reactively at 100 °C with a stirrer speed of 100 rpm. After 20 min, a white starch-PCL composite was obtained. The composite was equilibrated in a sealed plastic bag for 1 day before use. The composite consisting of corn starch (70 wt.%), PCLPU (10 wt.%) and PCL (20 wt.%) was designated as S70P20PU10. As a control, the same amount of PU powder was used to mix with starch/PCL by the same

133 procedure, and the resulting mixture was designated as S70P20PW10. With the same
134 nomenclature, the composite consisting of corn starch (70 wt.%), PCLPU (5 wt.%)
135 and PCL (25 wt.%) was designated as S70P25PU5. The composite consisting of corn
136 starch (70 wt.%) and PCL (30 wt.%) was designated as S70P30 and the composite
137 consisting of corn starch (70 wt.%), PCL (29 wt.%) and MDI (1 wt.%) was designated
138 as S70P29M1.

139 **Fractionation of the composites**

140 **Purification of starch-PCL composites**

141 To analyze the structure of the components in starch-PCL composites, PCL fraction
142 was first extracted from the composites using acetone. S70P20PU10 (10 g) and
143 acetone (200 g) were charged into a 500 mL three-necked flask fitted with a stirrer
144 operating at a speed of 300 rpm. The composite was dispersed at 55 ℃ for 1 h. After
145 the dispersion was centrifuged at 8000 rpm in a centrifuge machine (Shanghai Anting
146 Scientific Instrument Factory) for 10 min, the supernatant was PCL-acetone solution.
147 The acetone was then added into precipitate to further extract the PCL component
148 three times. After the PCL-acetone solution was concentrated, the concentrated PCL
149 and the precipitate were vacuum dried at 40 ℃ for 12 h to obtain extracted PCL
150 (APCL) and modified starch (CSPU), respectively. The procedure is illustrated in
151 Figure 1(a). With the above procedure, we also adopt the same method to extract PCL

from the composite S70P20PW10 using acetone. Finally the mixture of CS and PW (CSPW) was obtained.

Degradation of the composites

It was necessary to separate the PU component linked to starch to clarify the composition of CSPU. The starch matrix was therefore first degraded into water-soluble materials through the interaction of a starch enzyme, and the PU component was subsequently separated out. The detailed procedure was as follows: CSPU (6 g) and water (150 mL) were charged into a 250 mL three-necked flask fitted with a stirrer operating at a speed of 300 rpm. The temperature of the system was increased to 95 °C within 10 min to obtain starch dispersion. High-temperature amylase (0.2 g) was added into the flask at 95 °C to partially degrade the starch. 1 h after the addition of high-temperature amylase, the temperature of the system was decreased to 60 °C within 10 min and the pH value of the dispersion was adjusted to 4. The α-amylase (0.2 g) was then added. 2 h after the addition of the α-amylase, the viscosity of the dispersion decreased sharply. The dispersion contained only hydrophobic PU precipitate and degraded starch (DS) at this time. The dispersion was separated into a degraded starch solution and a precipitate in a centrifuge machine (Shanghai Anting Scientific Instrument Factory). The degraded starch solution was concentrated and freeze-dried to prepare degraded starch. To remove the existence of the enzyme

171 proteins in the precipitate, an aqueous NaOH solution was used to separate the
172 precipitate into a PU precipitate and a protein solution. The PU precipitate was then
173 washed and freeze-dried to obtain separated PU (SPU).[28] The procedure is illustrated
174 in Figure 1(b). S70P30 was also degraded to obtain DS and PCL component (EPCL)
175 using the same procedure. The specifications of the sample abbreviations were shown
176 in Table 1.

177 **Preparation of sample sheets by compression-molding**

178 Starch-PCL composites were compression-molded using a hot press (R3202 model,
179 Wuhan Qien Science & Technology Co., Ltd., Wuhan, China) equipped with a water
180 cooling system. The molding time, temperature and pressure were 5 min, 95 °C, and
181 40 MPa, respectively. The sheets were cut into dumbbell-like shapes (5A type)
182 according to GB/T1040-2006. The length of the dumbbell-like specimen was 75 mm,
183 and the width of the narrow section was 4 mm. The sheets were equilibrated at 60%
184 RH for at least 2 weeks before testing.

185 **Mechanical test**

186 The mechanical properties of the composites were assessed through tensile and impact
187 properties. The tensile properties were measured using a tensile tester (CMT6503,
188 Shenzhen SANS Test Machine Co. Ltd.). The samples cut from molded sheets were
189 aged at 60% RH and room temperature for 2 weeks. The tensile properties were then

190 measured using the tensile tester with a strain rate of 5 mm min^{-1}. The distance
191 between the two clamps was 40 mm. Strength at break (σ_b, MPa) and elongation at
192 break (ϵ_b, %) of the sheets were recorded. Five duplications were made. Impact
193 properties were measured using an impact tester (ZBC1400-1, Shenzhen SANS Test
194 Machine Co. Ltd.). Reversed notched Izod impact strength was measured by
195 following ASTM D256 recommendations, with five specimens for each sample (4.0
196 mm in thickness, 80 mm in length, and 10 mm in width). The specimen was held in a
197 vertical cantilever beam and broken by a pendulum (4 J). The specimen was impacted
198 on the side opposite to the notch. A notch was machined at an angle of 45° with a
199 depth of 0.25 mm.

200 **Fourier transform infrared spectroscopy (FTIR)**

201 A FTIR spectrometer (Avatar 360, Nicolet, MA, USA) was used at room temperature.
202 Test samples were pulverized with KBr and pressed into transparent disks for analysis.
203 The spectra of all the samples were recorded in transmission mode at a resolution of 4
204 cm^{-1} with accumulation of 8 scans.

205 **^{13}C CP/MAS NMR measurement**

206 Solid-state NMR experiment was carried out at B_0 = 9.4 T on a Bruker AVANCE III
207 400 WB spectrometer. The corresponding resonance frequency of ^{13}C was 100.6 MHz.
208 Samples were packed in a 4 mm ZrO_2 rotor and spun at the magic angle (54.7°). ^{1}H-

209 ^{13}C CP/MAS spectra were acquired with a contact time of 1.2 ms and a recycle delay
210 of 2 s. The ^{13}C chemical shift was externally referenced to the high field resonance of
211 hexamethylbenzene at 17.17 ppm.

212 **X-ray Diffraction (XRD)**

213 The composite powders were measured with wide angle X-ray diffraction (WAXRD)
214 (Y-2000 Dandong Radiative Instrument Group Ltd. CO., China). For irradiation, the
215 Cu Kα line was applied (λ at 0.1542 nm, cathode at 30 kV and 20 mA) and scattering
216 was recorded as 2θ in a range from 2 to 40º.

217 **Emission scanning electron microscopy (ESEM)**

218 An ESEM (FEI, Quanta 200 FEG, Netherlands) was used to observe the cross sections
219 of the fractured samples. Each sample was frozen using liquid nitrogen and then
220 fractured using tweezers to produce cross-sections. The cross-sections were coated
221 with gold and then used for ESEM observation.

222 **Differential scanning calorimetry (DSC)**

223 The DSC experiments (Diamond DSC, PerkinElmer Instruments, MA, USA) were
224 conducted in a nitrogenous atmosphere. The system was calibrated with indium and
225 about 10 mg of the sample was placed into an aluminum pan and sealed. The
226 specimens were heated from 30 to 110 °C at a rate of 20 °C min^{-1} (first heating scan),
227 then equilibrated at 110 °C for 2 min, cooled rapidly at 20 °C min^{-1} to -50 °C,

equilibrated at -50 °C for 2 min and finally heated again to 100 °C at 20 °C min^{-1} (second heating scan). The T_g was determined on the second scan at the midpoint of the calorific capacity change on the thermogram.

Thermal gravimetric analysis (TGA)

Testing was conducted using a thermal gravimetric analyzer (STA 449 C, NETZSCH Instruments Inc. MA, USA). Approximately 10 mg of the sample cut from the sheet was equilibrated at ambient conditions and then subjected to heating from 30 to 600 °C at a rate of 20 °C min^{-1} in a nitrogen atmosphere. The weight loss with respect to temperature and the maximum degradation temperature (T_{max}) of samples were recorded.

Dynamic mechanical analysis (DMA)

DMA was performed using a dynamic mechanical analyzer (DMA Q800, TA Instruments, DE, USA) in the single cantilever mode. Samples were investigated from –110 to 140 °C at a heating rate of 5 °C min^{-1}. A variable-amplitude sinusoidal tensile stress with a frequency of 1 Hz was applied to the samples to produce a sinusoidal strain of 15 μm amplitudes. The temperature at the peak of the tanδ curve ($T_{\tan \delta}$) was taken as the T_g of the samples.

Results and discussion

Structure

The FTIR spectra of corn starch (CS), degraded starch (DS), PCL, EPCL, APCL, CSPU and SPU are shown in Figure 2. As seen from Figure 2, the curves profile of CS was almost identical with that of DS. Generally, CS is known as a white powdered solid. However, DS appeared as a brown viscous liquid. These results indicated that the starch's intrinsic ring structure was preserved after the degradation process, which was in accord with the results obtained by Lv et al.[29] And there were no characteristic absorption peaks of urethane linkage (-NH-CO-O-) at 1732 cm^{-1} and 1644 cm^{-1} in the spectrum of DS, implying that PU was completely separated from starch. It could thus be determined that the starch was successfully degraded using the enzyme method. Moreover, similar spectra profiles were shown for PCL, APCL and EPCL. These results illustrated that PCL could be successfully separated from the composites through both the enzyme method and the acetone extraction method. In addition, comparing with the spectra of CSPU and SPU, a similar curves profile can be shown. The peaks for CSPU and SPU at 1644 cm^{-1} and 1732 cm^{-1} were attributed to the C-O and C=O groups in urethane linkage (-NH-CO-O-), respectively.[26,30] The broad peaks for CSPU and SPU at region of 3200–3400 cm^{-1} were dominated by the absorption of OH groups in starch component, and the intensity of this peak in SPU was decreased compared to CSPU. These results confirmed that the starch residues linked to PCLPU

through urethane linkages was difficult to degrade by enzyme though enzyme could degrade starch. It could thus be concluded that the PCLPU reacted with starch and the urethane linkages between them were stable.

The ^{13}C-NMR spectra of CSPU and CSPW are shown in Figure 3. The peak appeared at 35 ppm in CSPU and CSPW was ascribed to the polyurethane cross-linking, [31] which was formed in two ways in this research: the interaction between NCO groups in PCLPU and OH groups in starch granules; the interaction between NCO groups in MDI and OH groups in polycaprolactone diol. As shown in Figure 3, the peak at 35 ppm of CSPW was much weaker than that of CSPU. This confirmed that there were not only urethane bonds in PCLPU inherently but also the urethane linkages which were formed by PCLPU reacting with OH groups in starch granules in CSPU. Therefore, it could be concluded that urethane linkages existed between PCLPU and starch granules.

The WXRD spectra of S70P20PU10, S70P25PU5, S70P29M1 and S70P30 are shown in Figure 4. As shown in Figure 4, three peaks appeared at 15.2 º, 17.1 º and 18.1 º, which were attributed to a typical A-type diffraction pattern of starch crystal in the composites.[32] The peak at 22.1 º was associated with the V-type crystallinity of starch.[33] While the diffraction peaks at 21.4 º and 23.7 º were typical crystallization of PCL.[15] Compared with S70P30, the intensity of all peaks in other three samples was

decreased, which was ascribed to the incorporation of MDI or PUP. As the isocyanate groups of PUP or MDI reacted with the hydroxyl groups of starch, the interaction between the starch–starch chains declined accordingly. However, the interaction between the starch-PCL chains was increased. Consequently, the mobility of the starch and PCL chains were both limited, which resulted in a decrease in the crystallinity of starch and PCL in the blends.

The SEM micrographs of the fractured surfaces for S70P30, S70P29M1 and S70P20PU10 are shown in Fig. 5a-c. It could be observed that the starch granules in S70P30 [Fig. 5a] pulled out of their domains. Many empty cavities were shown in the PCL matrix. Moreover, a clear edge between the starch granules and PCL was observed, which indicated typical characteristics of an immiscible composite with poor interfacial adhesion. For S70P29M1 [Fig. 5b], a relatively smooth fracture surface was observed. Few starch particles pulled out and better interfacial adhesion produced by the MDI. As the isocyanate groups of MDI had reactivity with the hydroxyl groups of starch, MDI improved the compatibility between starch and PCL. A similar starch-PCL blends microstructure was observed by Yu et al., who concluded that the MDI compatibilizer improved the interface between starch and PCL.[18] However, S70P20PU10 showed a morphology indicating enhanced interfacial adhesion between PCL and starch, no cavities were observed on the fracture surface

[Fig. 5c]. The multifunctional PCLPU could efficiently react with starch through urethane linkages and was also compatible with the PCL continuous phase, which could be ascribed to their common PCL crystal soft segments structure (Scheme 1). Therefore, the compatibilizing effect of PCLPU was more significant compared to MDI.

In order to further investigate the effects of PCLPU on the starch-PCL composites, S70P30 and S70P20PU10 sheets were both immersed in the 1mol/L NaOH solution for 12h. The sheets were then dried at 40 °C and used for ESEM observation. Following the above procedure, the treated samples of S70P30 and S70P20PU10 were designated as D-S70P30 and D-S70P20PU10, respectively. The SEM images of D-S70P30 and D-S70P20PU10 are shown in Fig. 5d–e. As the starch dissolved in NaOH solution, the majority of the starch particles in D-S70P30 disbanded from the PCL matrix and left many voids [Fig. 5d], which indicated poor interfacial adhesion between PCL and starch. However, fewer starch granules pulled out from the PCL matrix in S70P20PU10 as compared to S70P30 [Fig. 5e]. It further demonstrated that PCLPU enhanced the interface compatibility between PCL and starch.

Figure 6 shows the typical DSC curves of the PCL/starch composites. The peak for S70P30 at 59.8 °C was attributed to the melting of the crystalline domains of the

PCL.[34] Compared with S70P30, the composite of S70P20PU10 with PCLPU exhibited its melting temperature (T_m) at about 62.4 °C. With the addition of the compatibilizer PCLPU, the value of T_m was higher than that of the virgin S70P30 composite. The interaction between PCL and PCLPU inhibited the molecular motion of PCL chains. As a result, the T_m value drifted to a higher temperature. Tsai et al. reported that the melting point of PCL soft segments in the PCLPU occurred at around 50 °C.[35] The PCL soft segments in the PCLPU could interact with PCL matrix through crystallinity, and the crystals formed between the PCLPU and PCL matrix were physical cross-linkers. Therefore, the compatibility between PCLPU layer and PCL matrix was improved. In S70P29M1, there was no this kind of PCL soft segment-PCL matrix interaction, and the compatibility between MDI and PCL matrix was improved limited.

The tan δ and storage modulus (E′) curves of S70P30 and S70P20PU10 are shown in Figure 7. Following the addition of PCLPU to starch-PCL blends, storage modulus was enhanced as the temperature increased from -100 to 40 °C and made the blends of S70P20PU10 more rigid than S70P30. This improvement could be attributed to the efficiency of the cross-link system, which included not only the physical cross-link between the PCLPU layer and PCL matrix through PCL crystals, but also the chemical cross-link between the PCLPU layer and starch through

342 urethane linkages. However, when temperature arrived above 40 °C, the storage
343 modulus of S70P20PU10 became lower than that of S70P30. This indicated that the
344 PCL crystals began to melt and the cross-links between the PCLPU layer and PCL
345 matrix thus collapsed, softening S70P20PU10. For the tan δ curves, the transition
346 peak of S70P30 was located at a low temperature between -50 °C to -10 °C, which
347 corresponded to the glass transition level of the PCL macromolecule.[36] However, an
348 increased glass transition temperature (T_g) was shown for S70P20PU10. This
349 phenomenon could be explained by the compatibilizing effect of PCLPU, which
350 strengthened the interaction between PCL and PCLPU and inhibited the free
351 molecular motion of PCL chains. The process of glass transition was thus slowed and
352 the value of T_g drifted to a higher temperature. This result was consistent with
353 previous observation of DSC. With the incorporation of PCLPU, the intensity of the
354 tan δ peak weakened, which could be attributed to the decreased content of the PCL
355 macromolecules from 30% to 20%. Furthermore, two different PCL structures were
356 detected in S70P20PU10: soft segment polyurethane (PCL diol) and PCL itself. As a
357 result, the peak shape of S70P20PU10 differed to S70P30.
358
359 **Mechanical Properties**
360 The mechanical properties of the composites were determined through tensile

and impact strength measurements and the subsequent results are listed in Table 2. In contrast with S70P30, the mechanical properties of S70P29M1 improved as a result of increased compatibility in the composites. As seen in Table 2, S70P25PU5 presented enhanced mechanical properties compared to S70P30. Moreover, the mechanical properties of the composites were increased with increasing PCLPU content. It was thus determined that the addition of PCLPU layer could not only improve the compatibility between PCL and starch, but also the mechanical properties of starch-PCL composites.

Thermal Properties

TGA and DTG thermograms of S70P30 and S70P20PU10 are shown in Figure 8. It could be found that the composites went through three stages degradation. The first stage began immediately after the temperature increased and ended at around 200 °C. During the first stage, a slight weight loss of around 5% was detected, which resulted from the vaporization of water in the composites. As shown in Figure 8, the residue weight of S70P20PU10 was higher than that of S70P30. In S70P30, the starch granules were surrounded by PCL matrix and the vaporization of the water could easily break through the PCL embedding layer. In S70P20PU10, the starch granules were not only enclosed by PCL matrix but also the PCLPU linkage layer, resulting in

less weight loss of the vaporization of water. The second stage corresponded to the thermal decomposition of starch macromolecules, which commenced at around 280 °C.[37] In the range of 350-390 °C, the remaining residue of S70P30 was higher than that of S70P20PU10, which was due to the decomposition of PCLPU. The degradation of the PU of urethane hard segment exactly occurred between the temperatures of 350 and 390 °C.[38] The third stage, the primary one, occurred between 350 and 500 °C, which corresponded to the thermal degradation of PCL.[39] This was exactly consistent with the PCL soft segments in PCLPU.[40] As shown in the DTG curves, the maximum degradation temperatures (T_{max}) of starch for S70P30 and S70P20PU10 were 310 °C and 320 °C, respectively. This indicated that S70P20PU10 exhibited better thermal stability than S70P30. Since the PCLPU enhanced the interphase interactions between PCL and starch, the thermal stability of S70P20PU10 was improved.

Conclusion

In this work, PU as a novel compatibilizer was successfully synthesized using PCL diol and MDI, then subjected for preparing starch-PCL composites in an intensive mixer. PU microparticles with multifunctional NCO groups reacted with starch through urethane linkages, which led to improved compatibility between starch and polyurethane. In addition, PCLPU was also compatible with PCL matrix, which

400 was attributed to the common components of PCL. Therefore, the compatibility of
401 starch-PCL composites was improved. The mechanical properties and the thermal
402 properties of the composites were improved compared to starch-PCL composites.
403 SEM observation also showed that interface between PCL and starch was enhanced
404 when PCLPU was mixed in the blends. Therefore, the multifunctional PCLPU was a
405 novel effective compatible interface to improve the compatibility of starch-PCL
406 composites.

407

408 **Acknowledgments**

409 The authors would like to express their appreciation for the financial support
410 from the National Natural Science Foundation of China under grant No. 50803024.

411

412

413

414

415

416 **References**

417 1 C. J. Pérez, V. A. Alvarez and A. Vázquez, *Mater. Sci. Eng.*, A, 2008, **480**, 259–
418 265.

2 E. Pérez, C. J. Pérez, V. A. Alvarez and C. Bernal, *Carbohydr. Polym.*, 2013, **97**, 269-276.

3 X. S. Wu, *J. Polym. Environ.*, 2011, **19**, 912-917.

4 A. R. Oromiehie, T. T. lari and A. Rabiee, *J. Appl. Polym. Sci.*, 2013, **127**, 1128-1134.

5 E. Landreau, L. Tighzert, C. Bliard, F. Berzin and C. Lacoste, *Eur. Polym. J.*, 2009, **45**, 2609-2618.

6 L. Vertuccio, G. Gorrasi, A. Sorrentino and V. Vittoria, *Carbohydr. Polym.*, 2009, **75**, 172-179.

7 P. Liu, L. Yu, H. S. Liu, L. Chen and L. Li, *Carbohydr. Polym.*, 2009, **77**, 250-253.

8 N. Wang, J. G. Yu and X. F. Ma, *Polym. Int.*, 2007, **56**, 1440-1447.

9 H. T. Liao and C. S. Wu, *Mater. Sci. Eng., A*, 2009, **515**, 207–214.

10 M. Joubert, C. Delaite, E. B. Lami and P. Dumas, *New J. Chem.*, 2005, **29**, 1601-1609.

11 Z. Q. Shen and J. L. Wang, *Bioresour. Technol.*, 2011, **102**, 8835–8838.

12 Q. X. Zhang, Z. Z. Yu, X. L. Xie, K. Naito and Y. Kagawa, *Polymer*, 2007, **48**, 7193–7200.

13 Y. Ikeo, K. Aoki, H. Kishi, S. Matsuda and A. Murakami, *Polym. Adv. Technol.*, 2006, **17**, 940-944.

14 S. Kalambur and S. S. H. Rizvi, *Polym. Eng. Sci.*, 2006, **46**, 650-658.

15 L. Chen, Z. Zhang, X. L. Zhuang, X. S. Chen, X. B. Jing, *J. Appl. Polym. Sci.*, 2010, **117**, 2724-2731.

16 M. A. Huneault and H. B. Li, *J. Appl. Polym. Sci.*, 2012, **126**, E96-E108.

17 J. F. Zhang and X. Z. Sun, *Biomacromolecules*, 2004, **5**, 1446-1451.

18 L. Yu, K. Dean, Q. Yuan, L. Chen and X. M. Zhang, *J. Appl. Polym. Sci.*, 2007, **103**, 812-818.

19 A. K. Sugih, J. P. Drijfhout, F. Picchioni, L. P. B. M. Janssen and H. J. Heeres, *J. Appl. Polym. Sci.*, 2009, **114**, 2315-2326.

20 E. J. Choi, C. H. Kim and J. K. Park, *J. Polym. Sci., Part B: Polym. Phys.*, 1999, **37**, 2430-2438.

21 R. Mani, J. Tang and M. Bhattacharya, *Macromol. Rapid Commun.*, 1998, **19**, 283-286.

22 Y. Peng, Z. Zheng, P. Y. Sun, X. L. Wang and T. K. Zhang, *New J. Chem.*, 2013, **37**, 729-734.

23 M. Ö. Seydibeyoğlu, M. Misra, A. Mohanty, J. J. Blaker, K.Y. Lee, A. Bismarck and M. Kazemizadeh, *J. Mater. Sci.*, 2013, **48**, 2167-2175.

24 H. X. Chen, M. S. Zheng, H. Y. Sun and Q.M. Jia, *Mater. Sci. Eng., A*, 2007, **445**, 725-730.

457 25 D. K. Chattopadhyay and K. V. S. N. Raju, *Prog. Polym. Sci.*, 2007, **32**, 352-418.

458 26 Y. Zhang, Y. M. Leng, M. Zhu, B. B. Fan, R. X. Yan and Q. X. Wu, *Carbohydr.*

459 *Polym.*, 2012, **88**, 1208-1213.

460 27 Z. M. Luo, Y. Zhang, H. B. Zhou, J. J. Liao, X. Zhang, Q. X. Wu, *New J. Chem.*,

461 2013, **37**,3109-3115.

462 28 Y. Zhang, Y. Huang, X. X. Chen, Z. S. Wu and Q. X. Wu, *Ind. Eng. Chem. Res.*,

463 2011, **50**, 11906-11911.

464 29 S. H. Lv, R. Gong and Y. F. Ma, *Polym. Adv. Technol.*, 2012, **23**, 1343-1349.

465 30 S. R. Yang, O. J. Kwon, D. H. Kim and J. S. Park, *Fiber. Polym.*, 2007, **8**, 257–

466 262.

467 31 J. S. Kim, T. S. Pathak, J. H. Yun, K. P. Kim, T. J. Park, Y. Kim and K. J. Paeng, *J.*

468 *Polym. Environ.*, 2013, **21**,224-232

469 32 W. L. Xie and L. Shao, *Starch/Stärke*, 2009, **61**, 702–708.

470 33 J. J. G. Van Soest and J. F. G. Vliegenthart, *Trends. Biotechnol.*, 1997, **15**, 208–213.

471 34 E. G. Kim, B. S. Kim and D. S. Kim, *J. Appl. Polym. Sci.*, 2007, **103**, 928-934.

472 35 H. C. Tsai, P. D. Hong and M. S. Yen, *Text. Res. J.*, 2007, **77**, 710-720.

473 36 L. Averous, L. Moro, P. Dole and C. Fringant, *Polymer*, 2000, **41**, 4157-4167.

474 37 X. X. Liu, L. Yu, H. S. Liu, L. Chen and L. Li, *Polym. Degrad. Stab.*, 2008, **93**,

475 260-262.

38 F. S. Chuang, *Polym. Degrad. Stab.*, 2007, **92**, 1393–1407.

39 A. Larrañaga and J. R. Sarasua, *Polym. Degrad. Stab.*, 2013, **98**, 751-758.

40 H. M. Jiang, Z. Zheng, W. H. Song, Z. M. Li and X. L. Wang, *Polym. Bull.*, 2007, **59**, 53–63.

Figure captions

Fig.1 (a). Schematic diagram of extracting PCL using acetone.

(b). Schematic diagram of degrading CSPU using enzyme.

Fig.2. FTIR spectra of CS, DS, PCL, EPCL, APCL, CSPU and SPU.

Fig.3. Solid state ^{13}C-NMR spectrum of CSPU and CSPW.

Fig.4. WXRD patterns of S70P30, S70P29M1, S70P25PU5 and S70P20PU10.

Fig.5. SEM micrographs of S70P30, S70P29M1, S70P20PU10, D-S70P30 and D-S70P20PU10.

Fig.6. DSC thermogram for S70P30 and S70P20PU10.

Fig.7. Tan δ and storage modulus (E′) curves of S70P30 and S70P20PU10.

Fig.8. TGA and DTG thermograms of S70P30 and S70P20PU10.

Scheme 1. Schematic diagram of the formation of compatible interface between PCL and starch filler

514

515 **Table.1.** Specifications of the sample abbreviations

516

Abbreviation	Specification	Abbreviation	Specification
PCL	Polycaprolactone	PCLPU	PCL-based polyurethane prepolymer
PW	PU powder	MDI	4, 4′-methylenedi-*p*-phenyl diisocyanate
CS	Corn starch	DS	Degraded starch
PUP	Polyurethane prepolymer	S70P30	Composite of starch/PCL (Mass ratio of CS and PCL is 70:30)
EPCL	Residue of S70P30 degraded by enzyme	S70P29M1	Composite of starch/PCL uses MDI as compatilizer (Mass ratio of CS, PCL and MDI is 70:29:1)
APCL	PCL extracted by acetone from S70P20PU10	S70P25PU5	Composite of starch/PCL uses PCLPU as compatilizer (Mass ratio of CS, PCLPU and PCL is 70:25:5)
CSPU	Residue of S70P20PU10 extracted by acetone	S70P20PU10	Composite of starch/PCL uses PCLPU as compatilizer (Mass ratio of CS, PCLPU and PCL is 70:20:10)
CSPW	Residue of S70P20PW10 extracted by acetone	D-S70P30	Residue of S70P30 extracted by NaOH
SPU	Residue of CSPU degraded by enzyme	D-S70P20PU10	Residue of S70P20PU10 extracted by NaOH

517

518

519

520

521

522

Table.2. Formulations of PCL/starch composites and the mechanical properties of molded composites sheets.

Sample	Formulations for composites				Tensile properties		Impact strength
	Starch (g)	PCL (g)	PCLPU (g)	MDI (g)	σ_b (MPa)	ϵ_b (%)	α_{iu} (KJ/M^2)
S70P30	49	21	0	0	3.8 ± 0.5	2.4 ± 1.2	1.5 ± 0.1
S70P29M1	49	20.3	0	0.7	13.8 ± 0.2	5 ± 0.5	4.6 ± 0.9
S70P25PU5	49	17.5	3.5	0	12.9 ± 0.6	7.5 ± 0.5	6.8 ± 0.5
S70P20PU10	49	14	7	0	17.8 ± 0.5	11.3 ± 2.8	12.7± 0.4

Fig.1(a). Schematic diagram of extracting PCL using acetone. APCL and CSPU represent extracted PCL with acetone and the residue after extracting PCL, respectively.

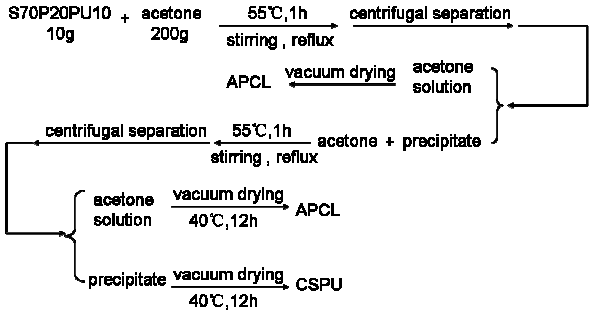

Fig.1(b). Schematic diagram of degrading CSPU using enzyme. S and P represent supernatant and precipitate, SPU and DS represent separated PU and degraded starch, respectively. HTA represents high-temperature amylase.

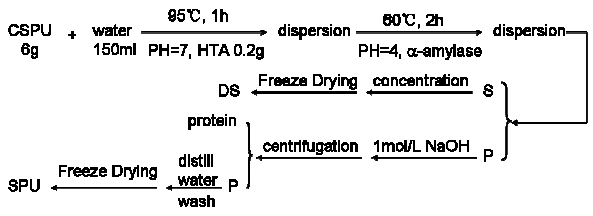

Fig.2. FTIR spectra of CS, DS, PCL, APCL, EPCL, CSPU, and SPU.

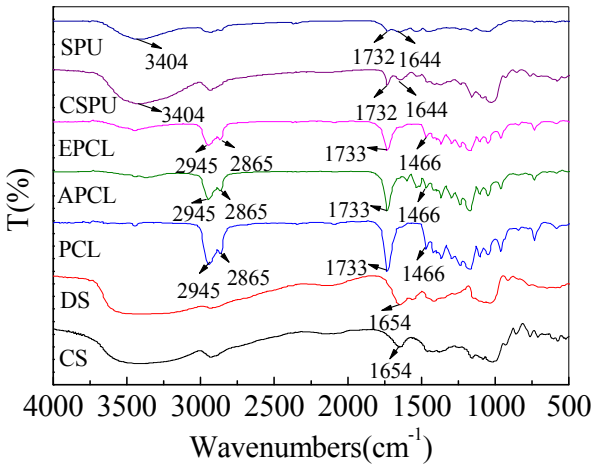

Fig.3. Solid state ^{13}C-NMR spectrum of CSPU and CSPW.

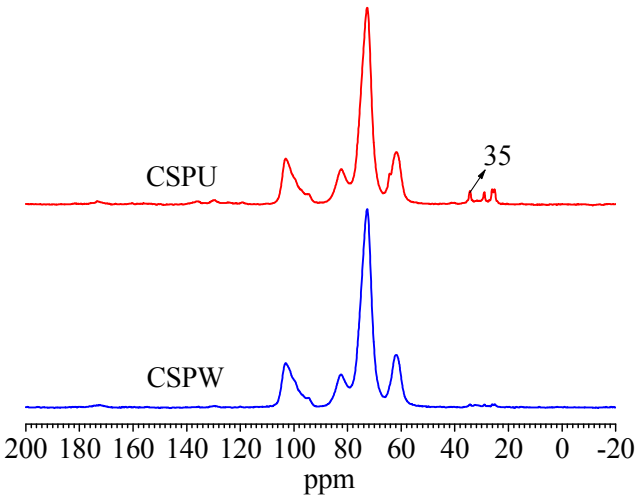

Fig.4. WXRD patterns of S70P30, S70P29M1, S70P25PU5 and S70P20PU10.

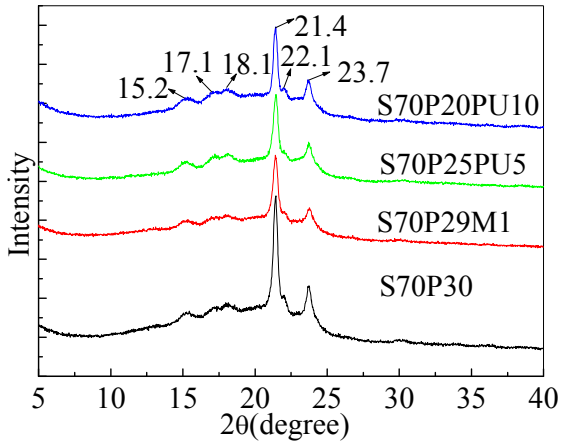

644

645 **Fig.5.** SEM micrographs of S70P30, S70P29M1, S70P20PU10, D-S70P30 and D-

646 S70P20PU10.

647

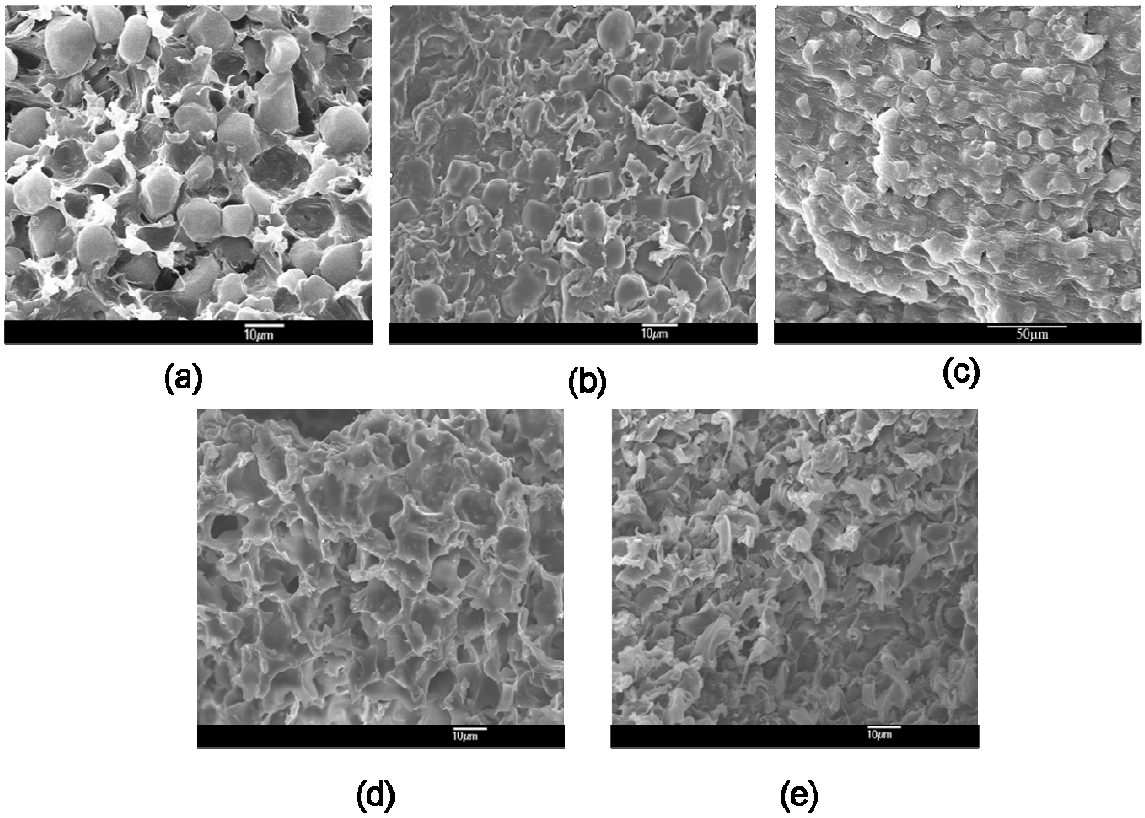

648

649

650

651

652 SEM images of: a) S70P30 (10.0KV, ×1000); b) S70P29M1 (10.0KV, ×1000); c)
653 S70P20PU10 (10.0KV, ×600); d) D-S70P30 (10.0KV, ×1000); and e) D-S70P20PU10
654 (10.0 KV, ×1000).

655

656

657

658

659

660

661

Fig.6. DSC thermogram for S70P30 and S70P20PU10.

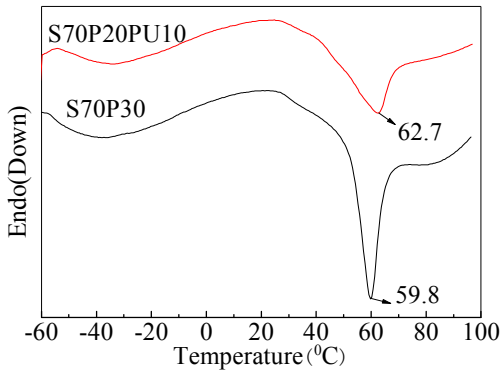

Fig.7. tan δ and storage modulus (E′) curves of S70P30 and S70P20PU10.

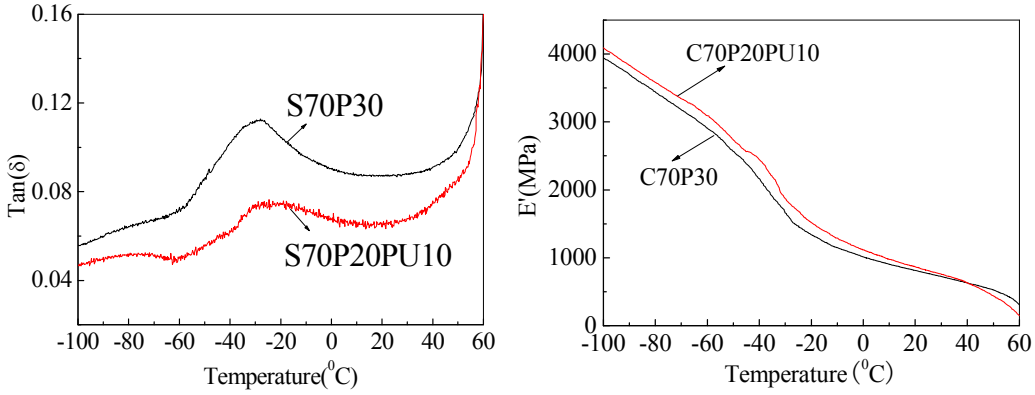

(a) (b)

Figure.8. TGA and DTG thermograms of S70P30 and S70P20PU10.

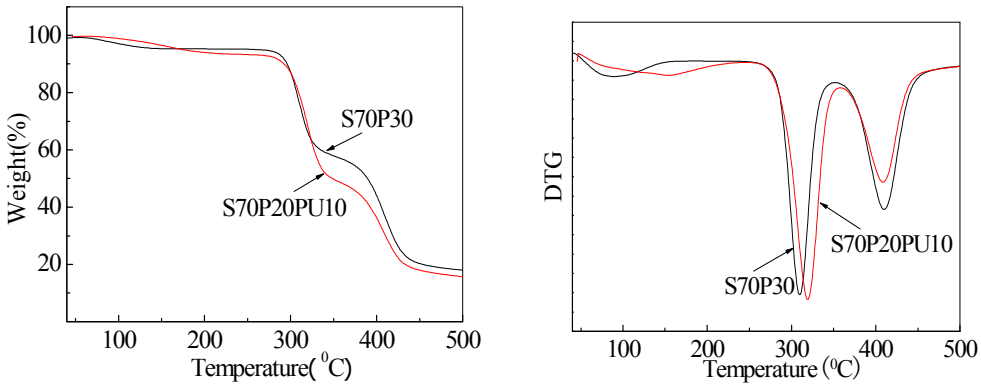

Scheme 1. Schematic diagram of the formation of compatible interface between PCL and starch filler.